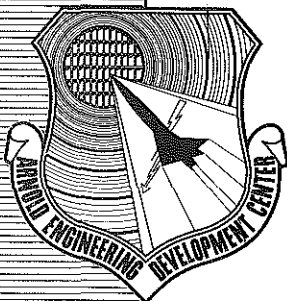


AEDC-TDR-62-206

*164*  
**ARCHIVE COPY  
DO NOT LOAN**



# **A CHECK CALIBRATION OF THE AEDC-PWT TRANSONIC MODEL TUNNEL**

**By**

**J. H. Nichols and F. M. Jackson  
Propulsion Wind Tunnel Facility  
ARO, Inc.**

**TECHNICAL DOCUMENTARY REPORT NO. AEDC-TDR-62-206**

**October 1962**

**AFSC Program Area 040A**

(Prepared under Contract No. AF 40(600)-1000 by ARO, Inc.,  
contract operator of AEDC, Arnold Air Force Station, Tenn.)

AEDC TECHNICAL LIBRARY



**ARNOLD ENGINEERING DEVELOPMENT CENTER  
AIR FORCE SYSTEMS COMMAND  
UNITED STATES AIR FORCE**

# NOTICES

Qualified requesters may obtain copies of this report from ASTIA. Orders will be expedited if placed through the librarian or other staff member designated to request and receive documents from ASTIA.

When Government drawings, specifications or other data are used for any purpose other than in connection with a definitely related Government procurement operation, the United States Government thereby incurs no responsibility nor any obligation whatsoever, and the fact that the Government may have formulated, furnished, or in any way supplied the said drawings, specifications, or other data, is not to be regarded by implication or otherwise as in any manner licensing the holder, or any other person or corporation, or conveying any rights or permission to manufacture, use, or sell any patented invention that may in any way be related thereto.

A CHECK CALIBRATION OF THE  
AEDC-PWT TRANSONIC MODEL TUNNEL

By  
J. H. Nichols and F. M. Jackson  
Propulsion Wind Tunnel Facility  
ARO, Inc.,  
a subsidiary of Sverdrup and Parcel, Inc.

October 1962  
ARO Project Nos. 240204 and 240305

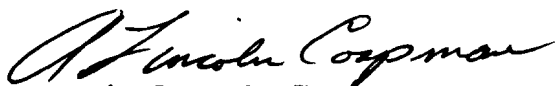


**ABSTRACT**

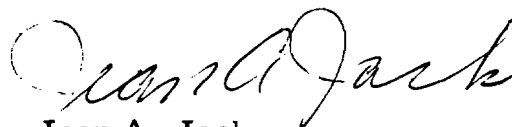
A brief investigation was conducted in the PWT Transonic Model Tunnel to check the validity of previous calibration results for two commonly used test section configurations. Static pressure measurements were made along the tunnel centerline and along the centerline of the top wall of the test section; simultaneous measurements of stilling chamber and plenum chamber pressures were obtained. The results of this investigation showed that the previous calibration results for a test section having four perforated walls was still correct, but previous results obtained with two perforated and two solid walls did not agree with those obtained in this investigation. This disagreement was felt to be caused by refinements in wall fabrication techniques and inaccuracies in the instrumentation used for the earlier investigation.

**PUBLICATION REVIEW**

This report has been reviewed and publication is approved.



A. Lincoln Coapman  
Major, USAF  
Acting AF Representative, PWT  
DCS/Test



Jean A. Jack  
Colonel, USAF  
DCS/Test



## CONTENTS

	<u>Page</u>
ABSTRACT . . . . .	iii
NOMENCLATURE . . . . .	vii
1.0 INTRODUCTION . . . . .	1
2.0 APPARATUS	
2.1 Transonic Model Tunnel . . . . .	1
2.2 Test Section Walls . . . . .	1
2.3 Instrumentation . . . . .	2
3.0 PROCEDURE . . . . .	2
4.0 RESULTS AND DISCUSSION . . . . .	3
5.0 CONCLUSIONS . . . . .	4
REFERENCES . . . . .	5

## ILLUSTRATIONS

Figure

1. Layout of the Transonic Model Tunnel . . . . .	6
2. Details of Test Section and Wall Geometry . . . . .	7
3. Nozzle Contour Used to Obtain Each Test- Section Mach Number . . . . .	8
4. Wall Angles Selected for Use at Each Test- Section Mach Number . . . . .	9
5. Tunnel Pressure Ratio Used to Obtain Each Test-Section Mach Number . . . . .	10
6. Variation of Reynolds Number and Stagnation Temperature with Mach Number . . . . .	11
7. Centerline Mach Number Distributions with Four Perforated Test-Section Walls	
a. $M = 0.60$ to $1.025$ . . . . .	12
b. $M = 1.05$ to $1.50$ . . . . .	13
8. Centerline Mach Number Distributions with Two Perforated Test-Section Walls at $\theta_w = 0$	
a. $M = 0.60$ to $1.025$ . . . . .	14
b. $M = 1.05$ to $1.50$ . . . . .	15
9. Top Wall Mach Number Distributions with Four Perforated Test-Section Walls	
a. $M = 0.60$ to $1.025$ . . . . .	16
b. $M = 1.05$ to $1.50$ . . . . .	17

<u>Figure</u>	<u>Page</u>
10. Top Wall Mach Number Distributions with Two Perforated Test-Section Walls at $\theta_w = 0$	
a. $M = 0.60$ to $1.025$ . . . . .	18
b. $M = 1.05$ to $1.50$ . . . . .	19
11. Comparison of Present and Previous Calibration Results with Four Perforated Test-Section Walls. . . . .	20
12. Comparison of Present and Previous Calibration Results with Two Perforated Test-Section Walls at $\theta_w = 0$ . . . . .	23



## NOMENCLATURE

$M$	Local Mach number
$M_{\infty}$	Free-stream Mach number
$p_c$	Plenum chamber static pressure, psf
$p_t$	Stilling chamber total pressure, psf
$\theta_w$	Angle of the top and bottom test-section walls, positive when walls are diverged, min
$\lambda$	Ratio of the stilling chamber total pressure to the static pressure downstream in the diffuser



## 1.0 INTRODUCTION

The Transonic Model Tunnel, Propulsion Wind Tunnel Facility (PWT), Arnold Engineering Development Center (AEDC), Air Force Systems Command (AFSC), has a test section 12 by 12 inches in cross section and 37.5 inches in length, made up of removable walls. The availability of both perforated and glass sidewalls plus extra wall liner material makes this tunnel readily adaptable to a wide variety of tests. Although the tunnel was calibrated earlier with both two and four perforated wall configurations, the question of calibration changes has arisen several times when greater than normal precision has been desired. To answer these questions, the brief check calibration reported herein was conducted.

## 2.0 APPARATUS

### 2.1 TRANSONIC MODEL TUNNEL

The Transonic Model Tunnel is a continuous-flow non-return wind tunnel equipped with a two-dimensional flexible nozzle and a plenum evacuation system, resulting in a test-section Mach number range from 0.60 to 1.50. The general arrangement of the tunnel and its associated equipment is shown in Fig. 1. A detailed description of the tunnel and its capabilities are given in Ref. 1.

### 2.2 TEST SECTION WALLS

Two wall configurations are frequently used to form the 12-in. by 12-in. by 37.5-in. test section. For force and pressure distribution tests, four perforated walls are used; the perforated wall liners are 1/8-in. thick and have 1/8-in. -diam holes with the axes of the holes inclined into the airstream at an angle of 60 deg. The ratio of open to total area is six percent. A general arrangement of the test section and the perforated wall geometry is shown in Fig. 2. A linear variation in the distribution of the perforated openings extends from the nozzle exit to a station 10 in. downstream (as indicated in Fig. 2) to provide for smooth transition in the development of supersonic flow. The top and bottom walls are supported by flexures at the nozzle exit and screw actuators

---

Manuscript released by authors October 1962.

at the downstream end to provide for wall angle adjustments. The side-walls are not adjustable and are parallel.

For tests requiring flow visualization over large areas, solid side-walls of 3/4-in. glass are used in conjunction with the normal perforated top and bottom walls. Large windows in the sides of the plenum chamber provide excellent viewing of the entire test section when these walls are used.

## 2.3 INSTRUMENTATION

A 1-in. -diam static pressure probe, extending from the rear of the test section upstream into the stilling chamber to eliminate nose disturbances, was used to obtain the centerline static pressure distributions. This installation is illustrated in Fig. 2. Static orifices installed along the centerline of the top perforated wall were used to obtain wall static pressure distributions. The centerline tube orifices were connected to a manometer board with tetrabromoethane (TBE) as the measuring fluid and with the plenum chamber pressure ( $p_c$ ) as the reference pressure. This reference pressure was read accurately from an Ideal mercury manometer. The wall static pressures, stilling chamber total pressure ( $p_t$ ), a vacuum reference, and  $p_c$  were displayed on a mercury manometer which had  $p_t$  as the reference pressure. This combination results in faster data reduction because by setting the difference between  $p_t$  and vacuum equal to unity on the film reader, the ratio of local static pressure to  $p_t$  can be read directly. The stilling chamber total pressure ( $p_t$ ) was also displayed on a Wallace and Tiernan pressure gage on the control console, where it was used along with  $p_c$  from the Ideal manometer to set the desired test conditions.

## 3.0 PROCEDURE

In order to keep the tunnel occupancy time required for a check calibration to a minimum the conditions for which data were obtained were selected to represent those most commonly used in testing. The full Mach number range of 0.60 to 1.50 was investigated for both of the wall configurations normally used. The sonic nozzle contour was used in conjunction with plenum suction to establish test-section Mach numbers up through 1.15; higher Mach numbers were obtained by using contoured nozzle settings (see Fig. 3) with plenum suction to aid in stabilizing test-section flow. With four perforated walls installed, the top and bottom wall angles were varied as shown in Fig. 4, using settings which were found to minimize interference in earlier investigations (Ref. 2). With the solid

sidewalls installed, the top and bottom walls were kept parallel. The tunnel pressure ratios ( $\lambda$ ) selected were also based on previous investigations and operating experience; these are shown in Fig. 5. Tunnel stagnation pressure ( $p_t$ ) varied from 2795 to 2930 psf during this calibration period. Stagnation temperature was varied (Fig. 6) to prevent visible moisture condensation at the higher Mach numbers. These variations in tunnel conditions resulted in the Reynolds numbers shown in Fig. 6.

#### 4.0 RESULTS AND DISCUSSION

The data obtained during this check calibration are presented as Mach number distributions along the test-section centerline and along the top wall centerline. The distributions along the test-section centerline with four perforated walls installed are shown in Fig. 7; symbols are used to denote the value of  $\theta_w$  for each curve. At Mach number 1.025 data were obtained at two wall angles because of the abrupt change in the wall angle schedule between Mach numbers 1.00 and 1.025, shown in Fig. 4. Very little difference was noted in the flat portion of the distribution as the walls were converged 40 min (Fig. 7a). The centerline distributions obtained with two perforated and two solid walls at  $\theta_w = 0$  are shown in Fig. 8. Figures 9 and 10 present the Mach number distributions measured along the top wall for the two wall configurations investigated.

To compare these results with previous calibration results, the centerline Mach number distributions between stations 11.7 and 29.7 were used to determine the average centerline Mach number, or free-stream Mach number for the testing region,  $M_\infty$ . Figures 11 and 12 present the relationships between  $M_\infty$  and  $p_c/p_t$  as determined during this investigation and show comparisons with the previous calibration results. In the case of the test section with four perforated walls (Fig. 11), the data points obtained in this investigation agreed quite well with the more extensive curves obtained previously in 1958, thereby substantiating the previous calibration results. With two perforated and two solid walls, the results of this investigation differed from the earlier calibration by significant amounts, ranging from  $\Delta M = 0.008$  at the lower Mach numbers to  $\Delta M = 0.020$  at the upper Mach numbers. These previous results were from a 1957 calibration using an early set of walls which were of the same basic design but lacked some of the fabrication refinements incorporated in later walls. It is felt that differences in the walls themselves caused part of this disagreement, and that inaccuracies in instrumentation used for the early calibration probably account for the remainder of the difference in results. Because all of the results of this investigation,

both with four perforated and two perforated walls, were obtained with the same instrumentation and the same physical walls, it is felt that these results are the more nearly correct and will therefore be used for future test work.

In the region normally used for model testing, between stations 11.7 and 29.7, the Mach number deviations from the mean were found to be as follows:

Four Perforated Walls

$M_\infty < 1.0$	$\Delta M = \pm 0.003$
$M_\infty > 1.0$	$\Delta M = \pm 0.015$

Two Perforated Walls

$M_\infty < 1.0$	$\Delta M = \pm 0.002$
$M_\infty > 1.0$	$\Delta M = \pm 0.015$

From a study of the measuring equipment and the results obtained during this investigation, the uncertainties in the data presented were estimated for a probability of 95 percent. These uncertainties are given in the following table:

$\frac{\Delta M}{\phantom{0.003}}$	$\frac{\Delta(p_c/p_t)}{\phantom{0.002}}$	$\frac{\Delta \lambda}{\phantom{0.002}}$	$\frac{\Delta \theta_w}{\phantom{\pm 2 \text{ min}}}$
$\pm 0.003$	$\pm 0.002$	$\pm 0.002$	$\pm 2 \text{ min}$

## 5.0 CONCLUSIONS

From this check calibration, the following conclusions have been reached:

1. The previous calibration results for a test section having four perforated walls are still valid and may be used with confidence for future tests.
2. The previous calibration results for a test section having two perforated and two solid walls cannot be used with the perforated walls presently in use; the calibration results presented in this report are recommended for use with this test section configuration.

## REFERENCES

1. Test Facilities Handbook, (4th Edition). "Propulsion Wind Tunnel Facility, Vol. 3." Arnold Engineering Development Center, July 1962.
2. Chew, William L. "Determination of Optimum Operating Parameters for the 1-Foot Transonic Tunnel Utilizing Cone-Cylinder Bodies of Revolution." AEDC-TN-60-69, April 1960.

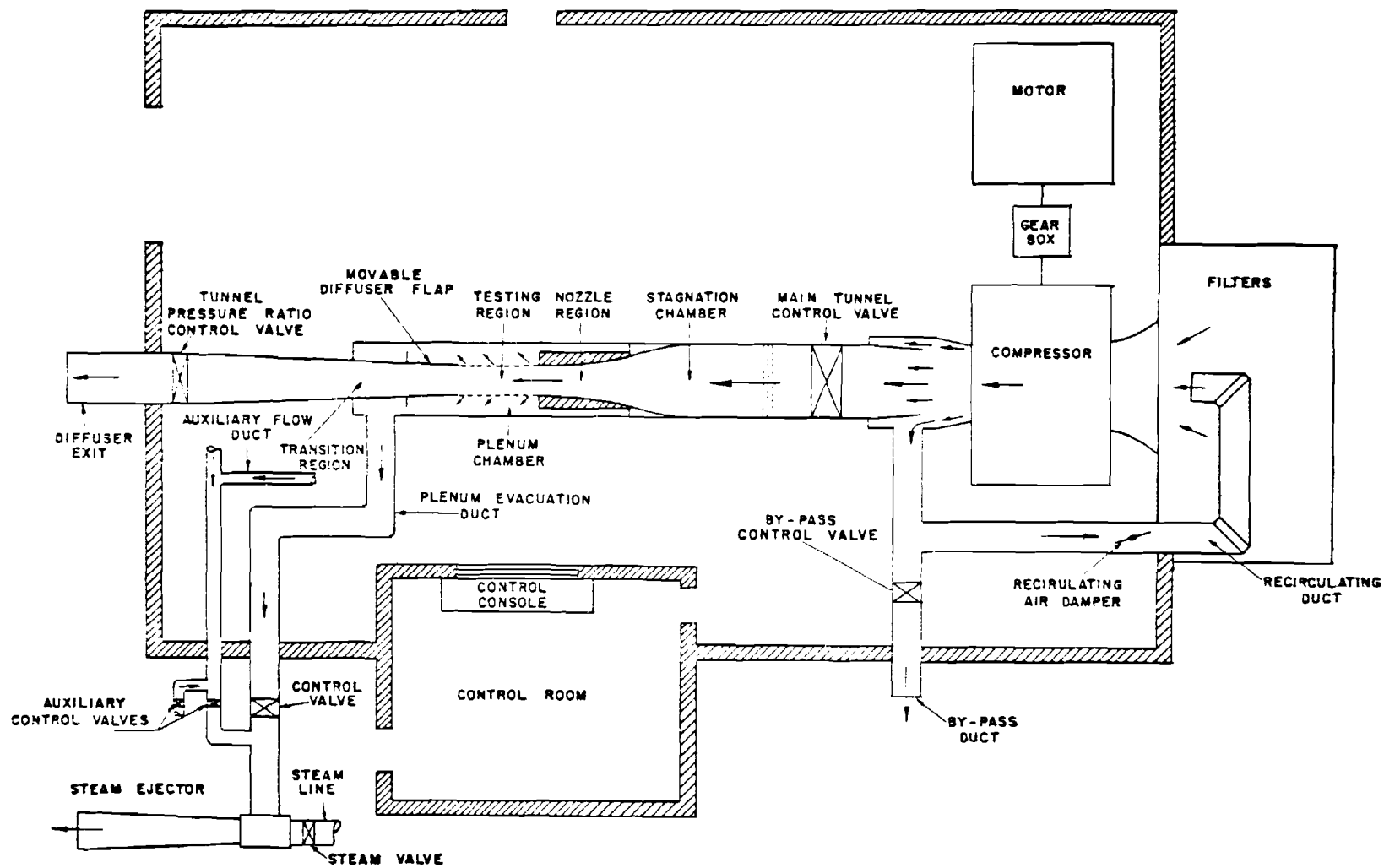


Fig. 1 Layout of the Transonic Model Tunnel



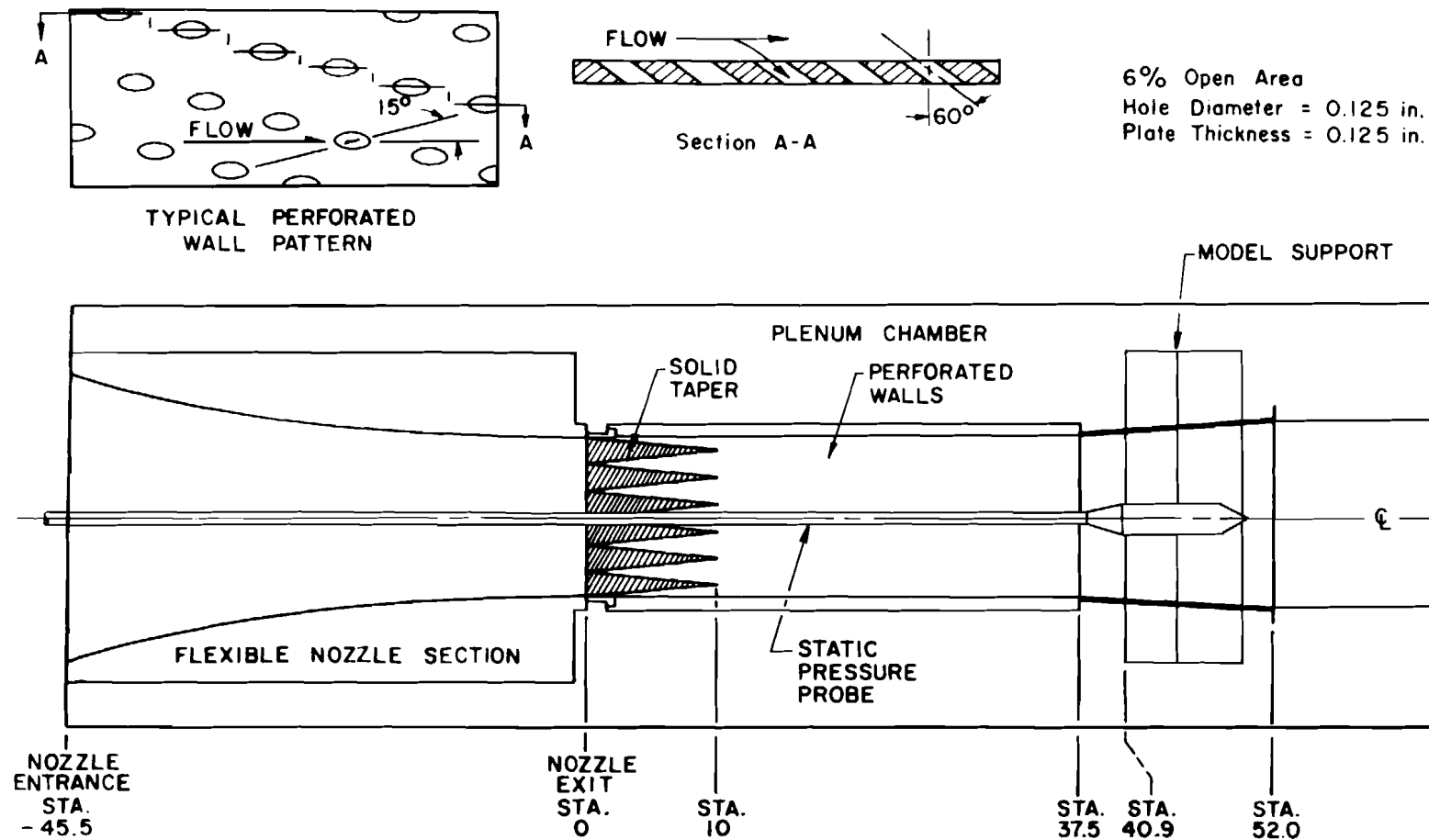


Fig. 2 Details of Test Section and Wall Geometry

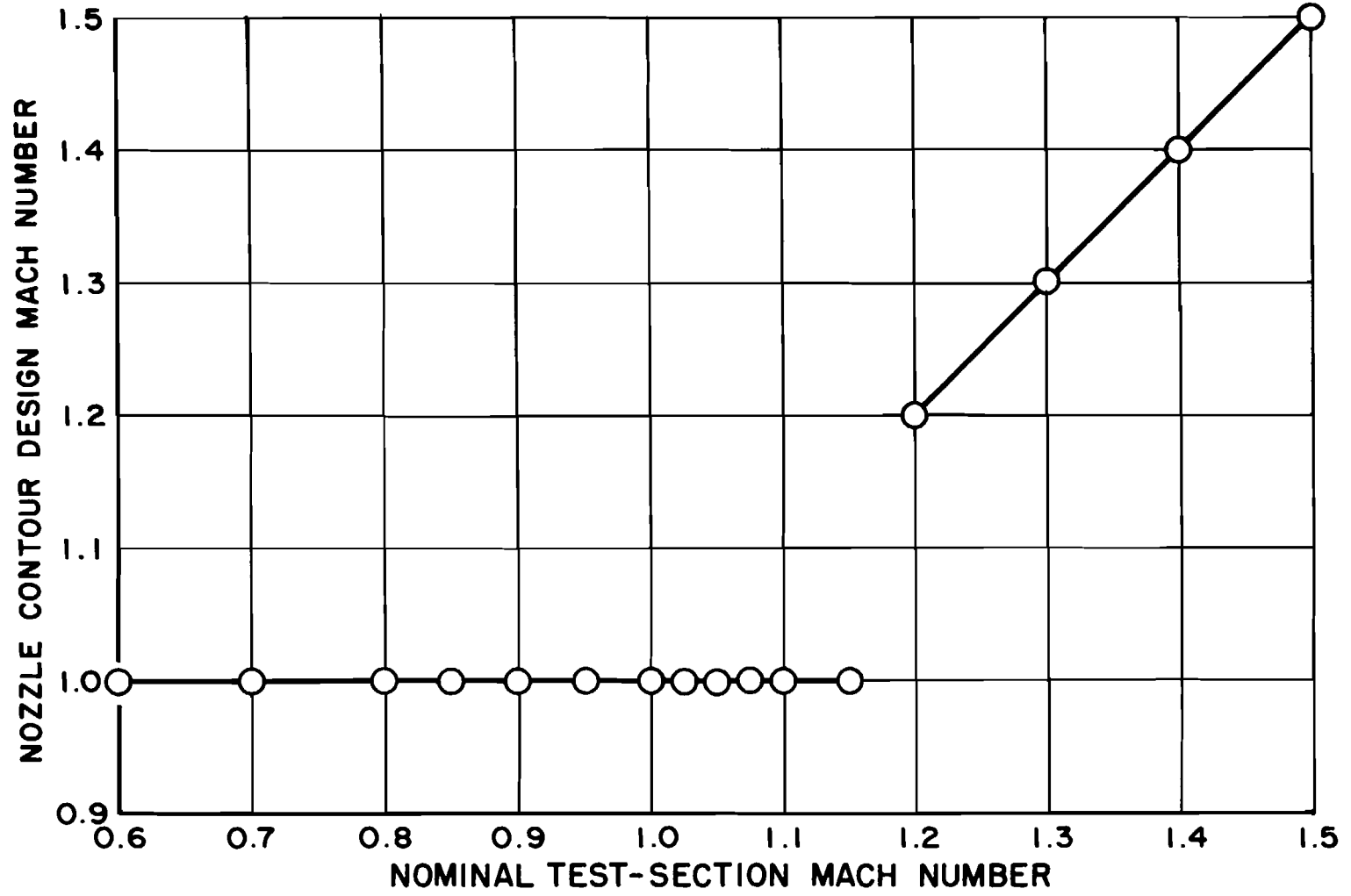


Fig. 3 Nozzle Contour Used to Obtain Each Test-Section Mach Number

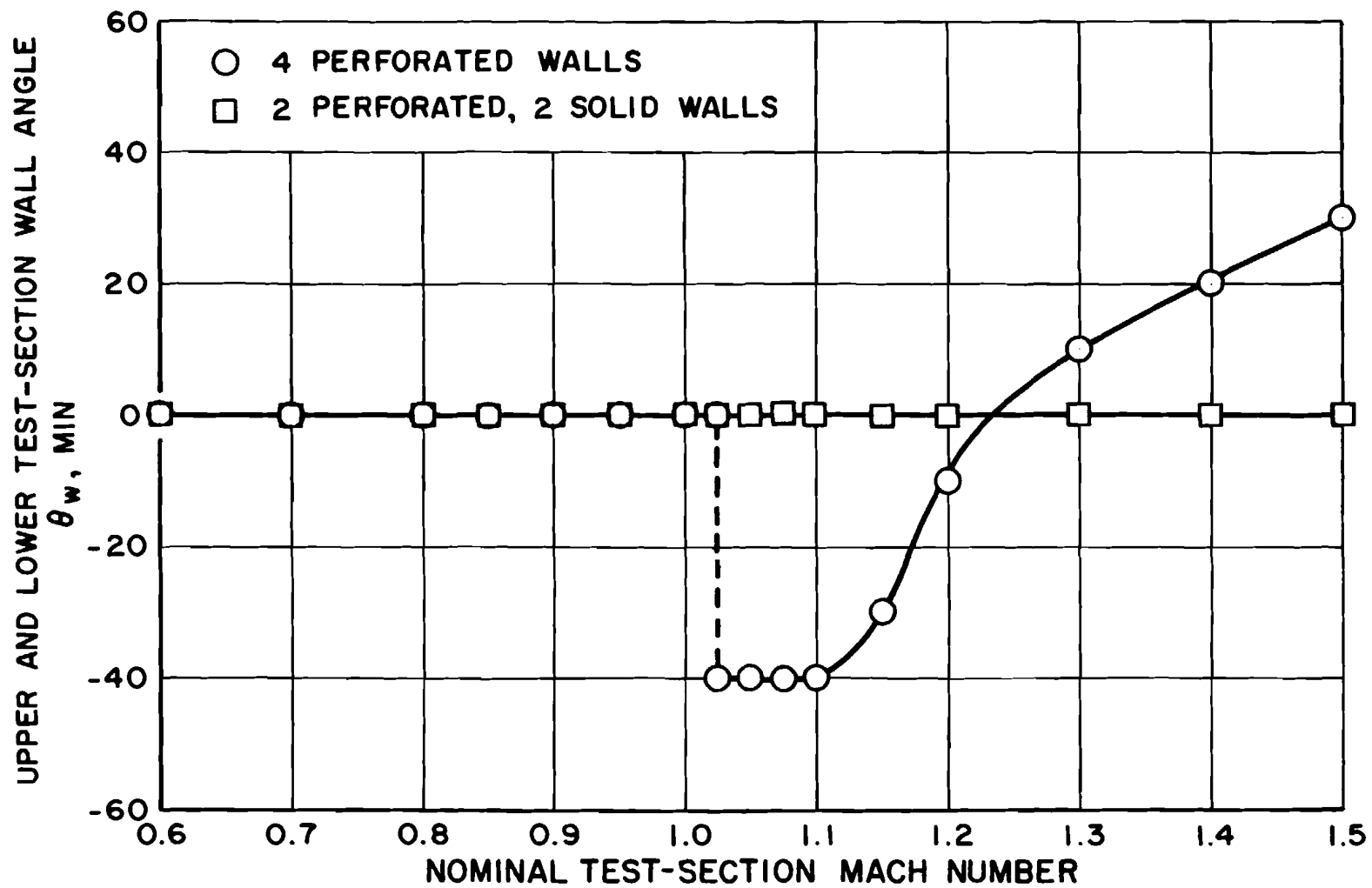


Fig. 4 Wall Angles Selected for Use at Each Test-Section Mach Number

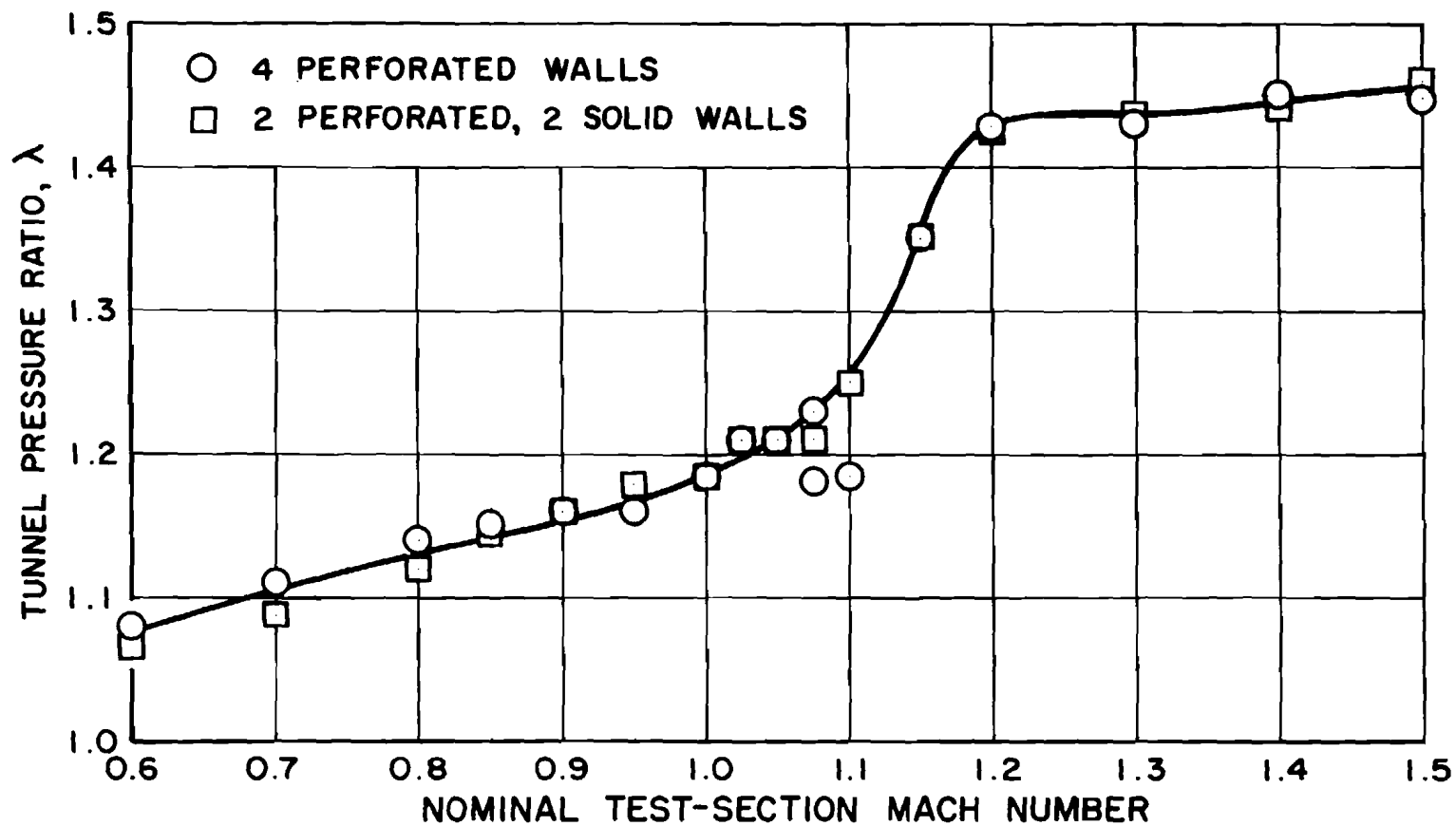


Fig. 5 Tunnel Pressure Ratio Used to Obtain Each Test-Section Mach Number

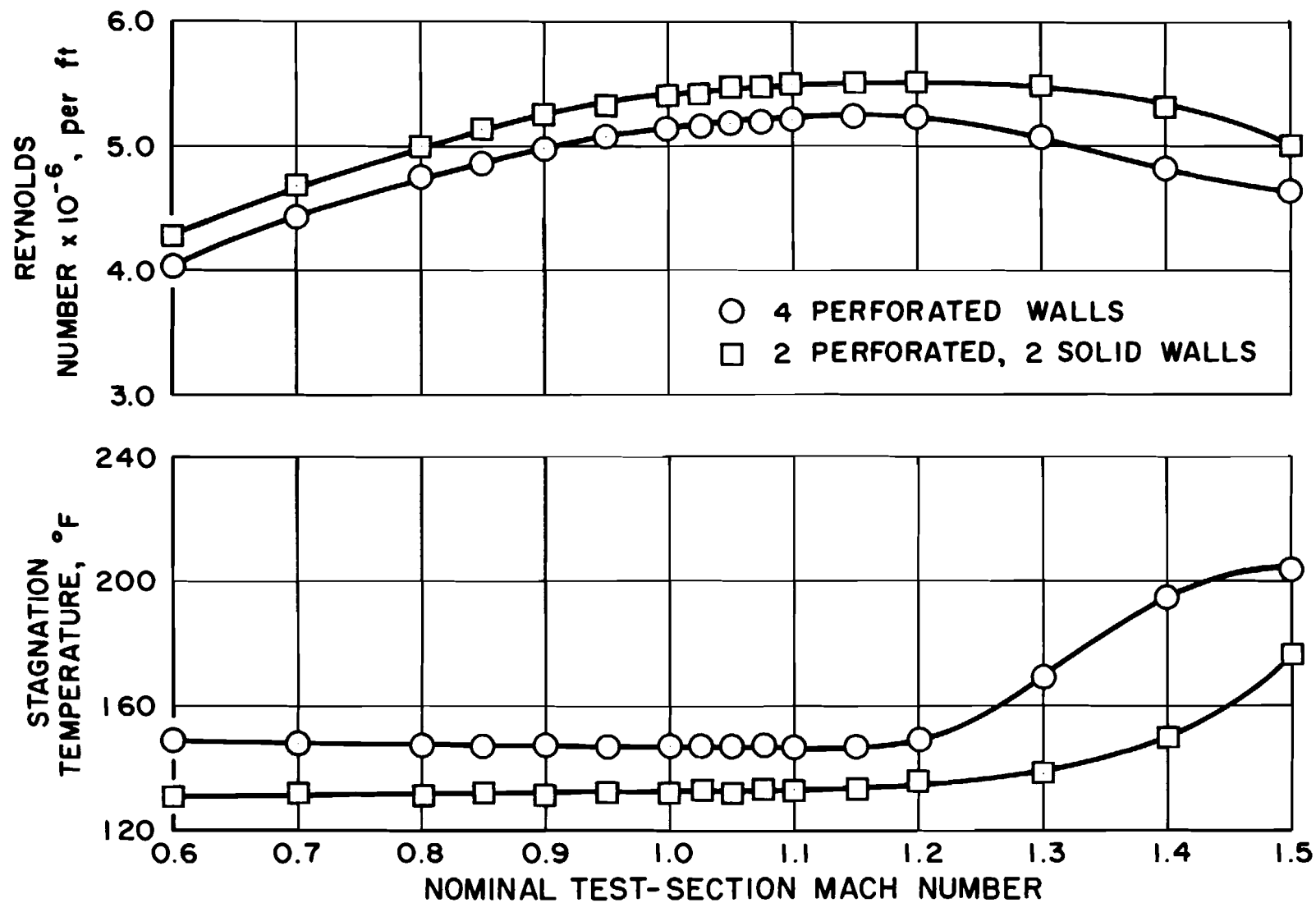


Fig. 6 Variation of Reynolds Number and Stagnation Temperature with Mach Number

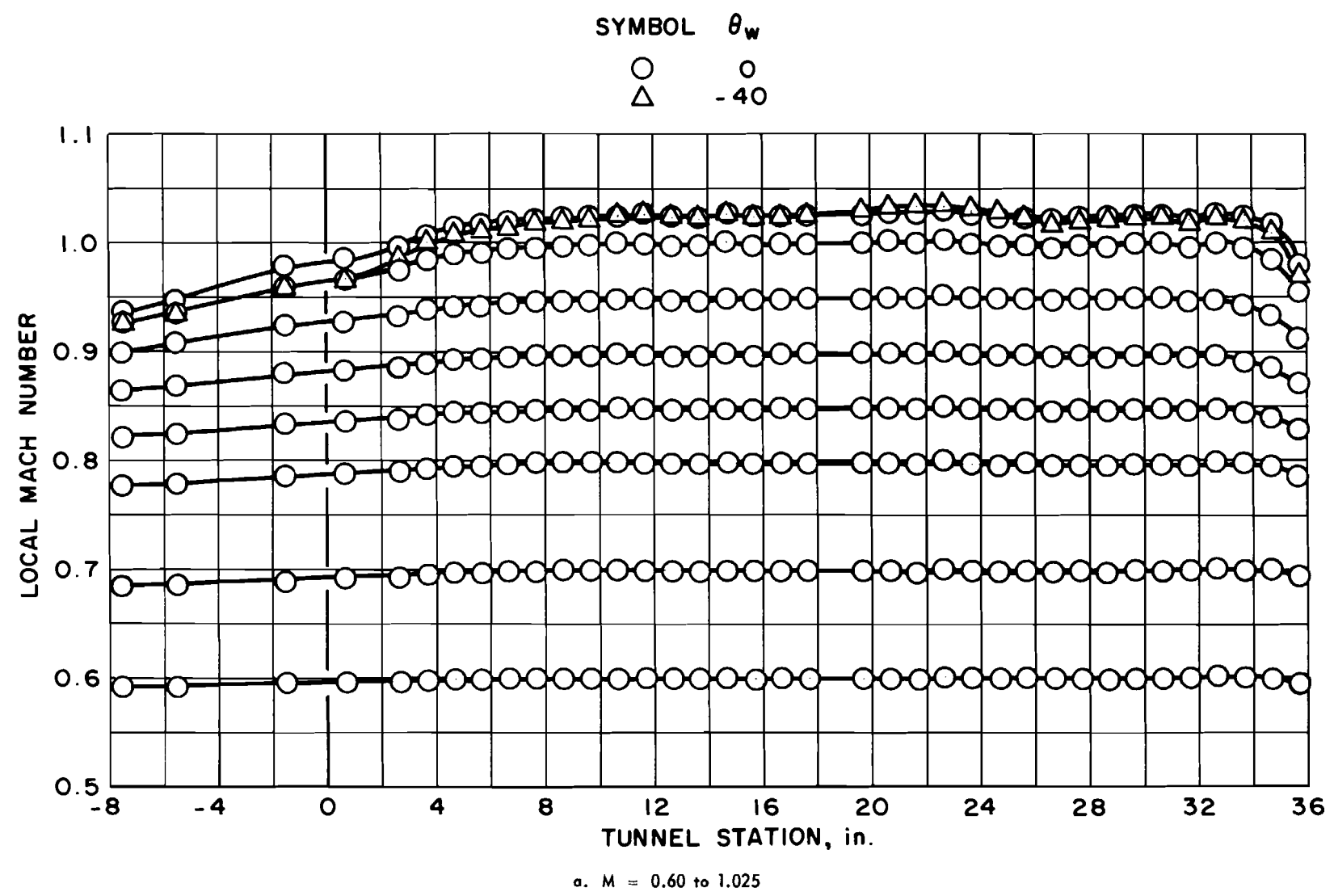
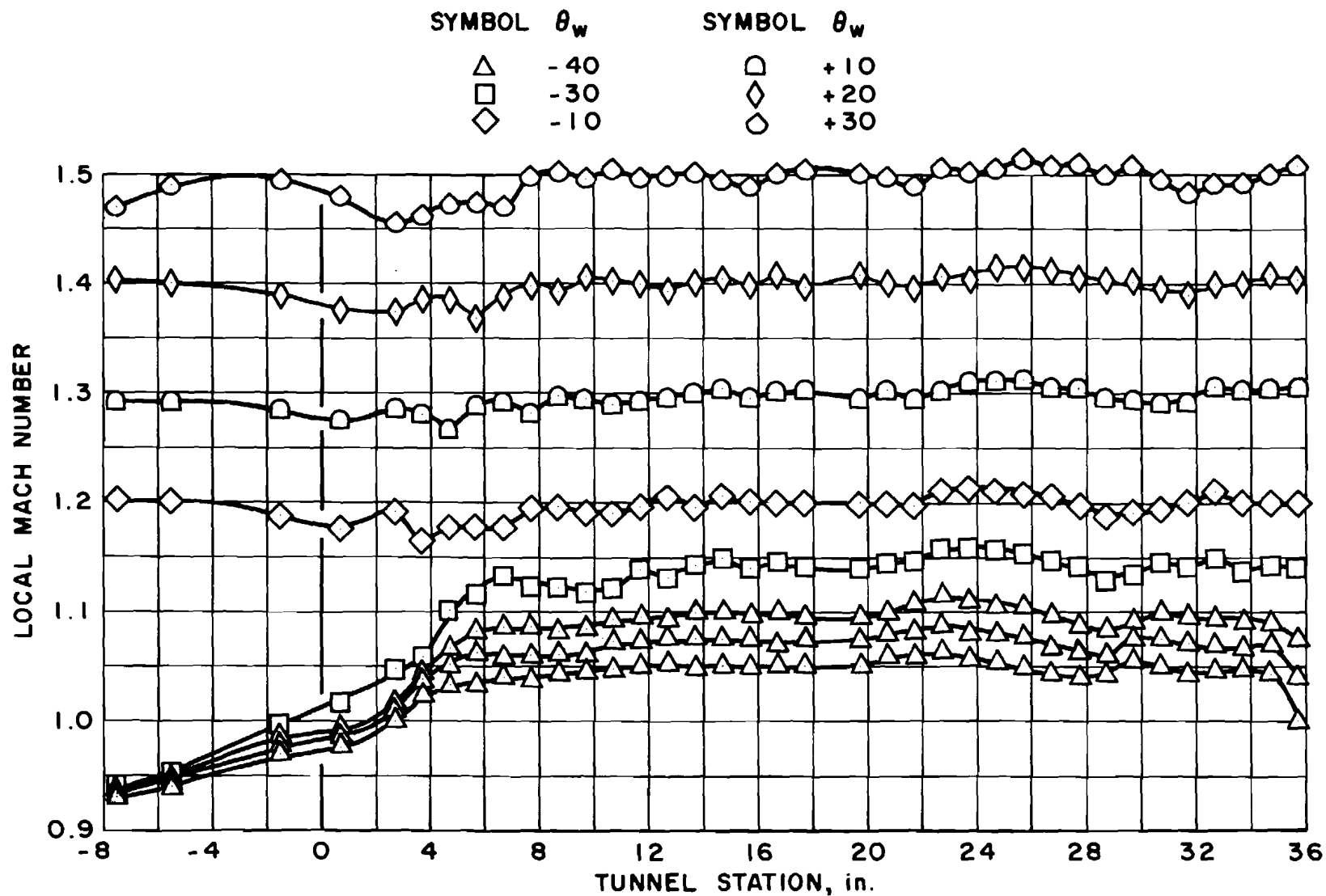
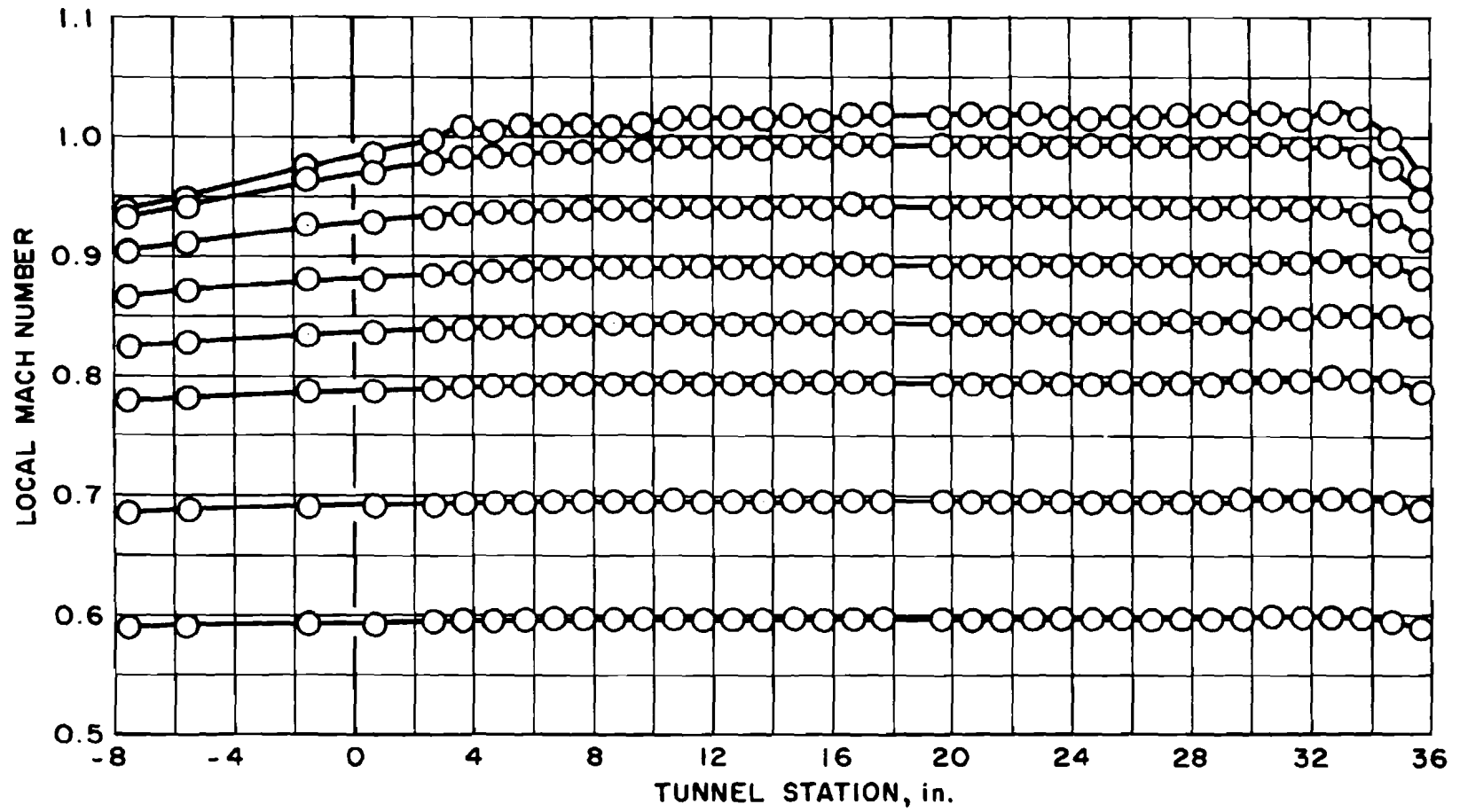


Fig. 7 Centerline Mach Number Distributions with Four Perforated Test-Section Walls



b.  $M = 1.05$  to  $1.50$

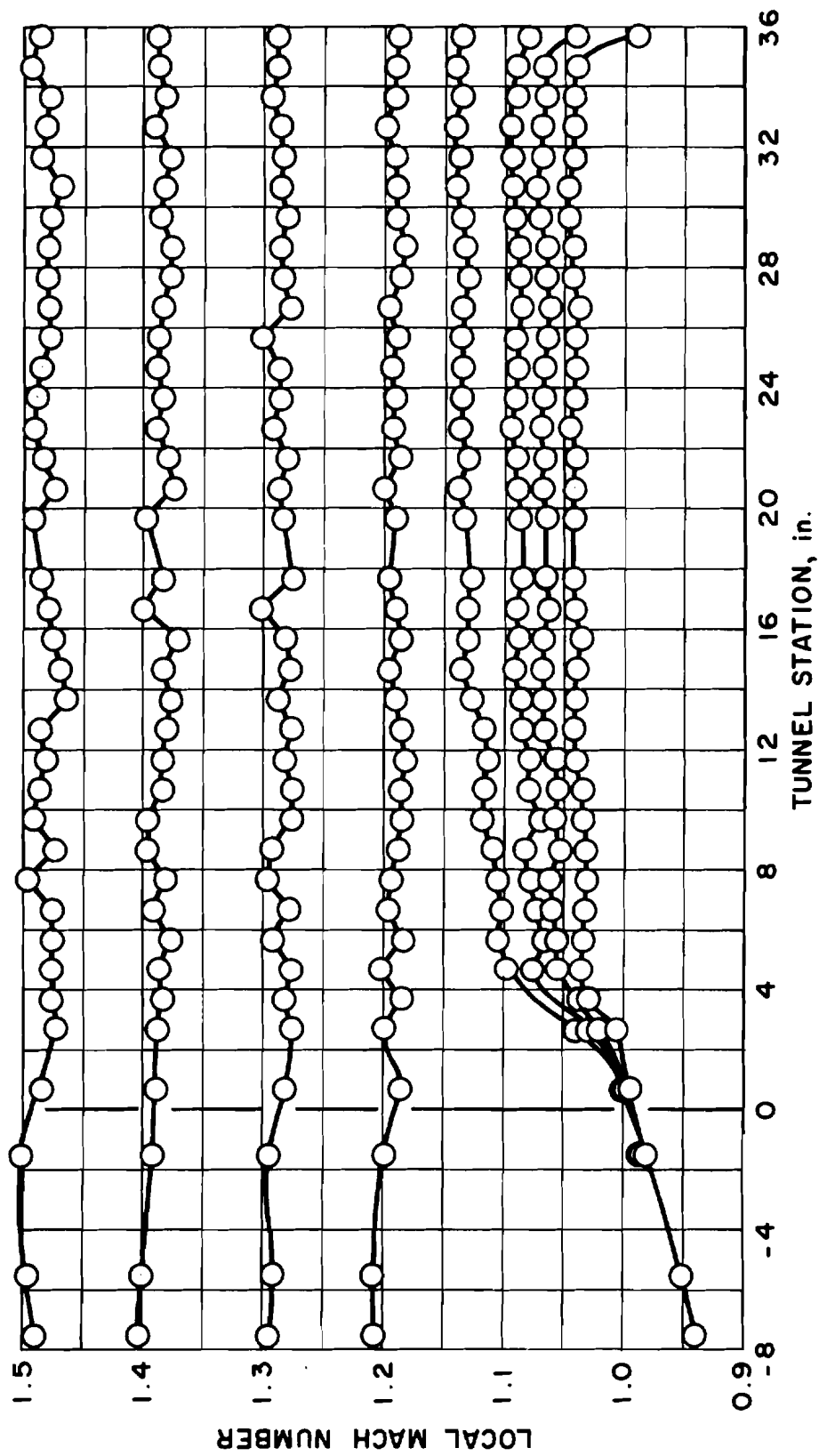
Fig. 7 Concluded



a.  $M = 0.60$  to  $1.025$

Fig. 8 Centerline Mach Number Distributions with Two Perforated Test-Section Walls at  $\theta_w = 0$





b.  $M = 1.05$  to  $1.50$

Fig. 8 Concluded

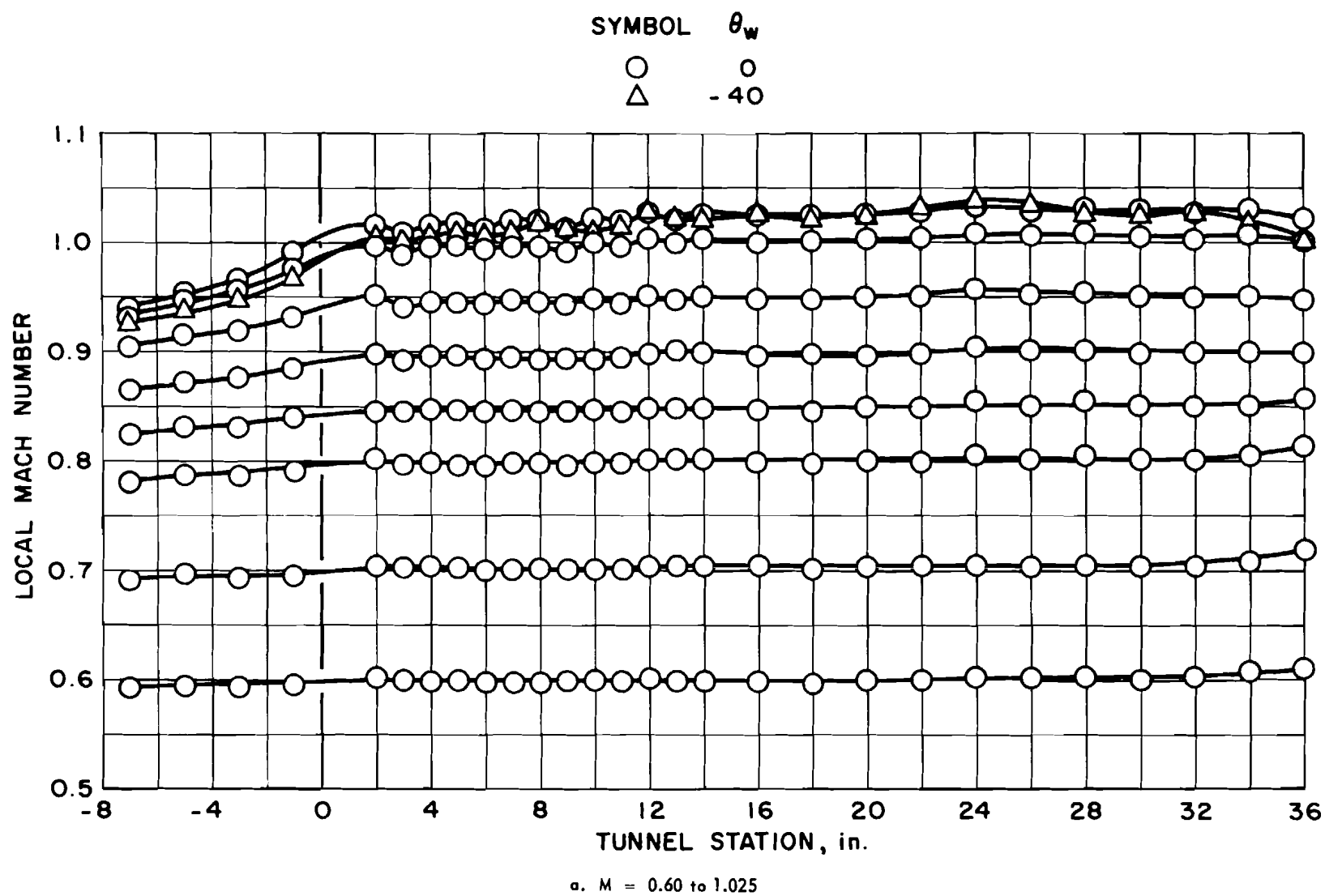
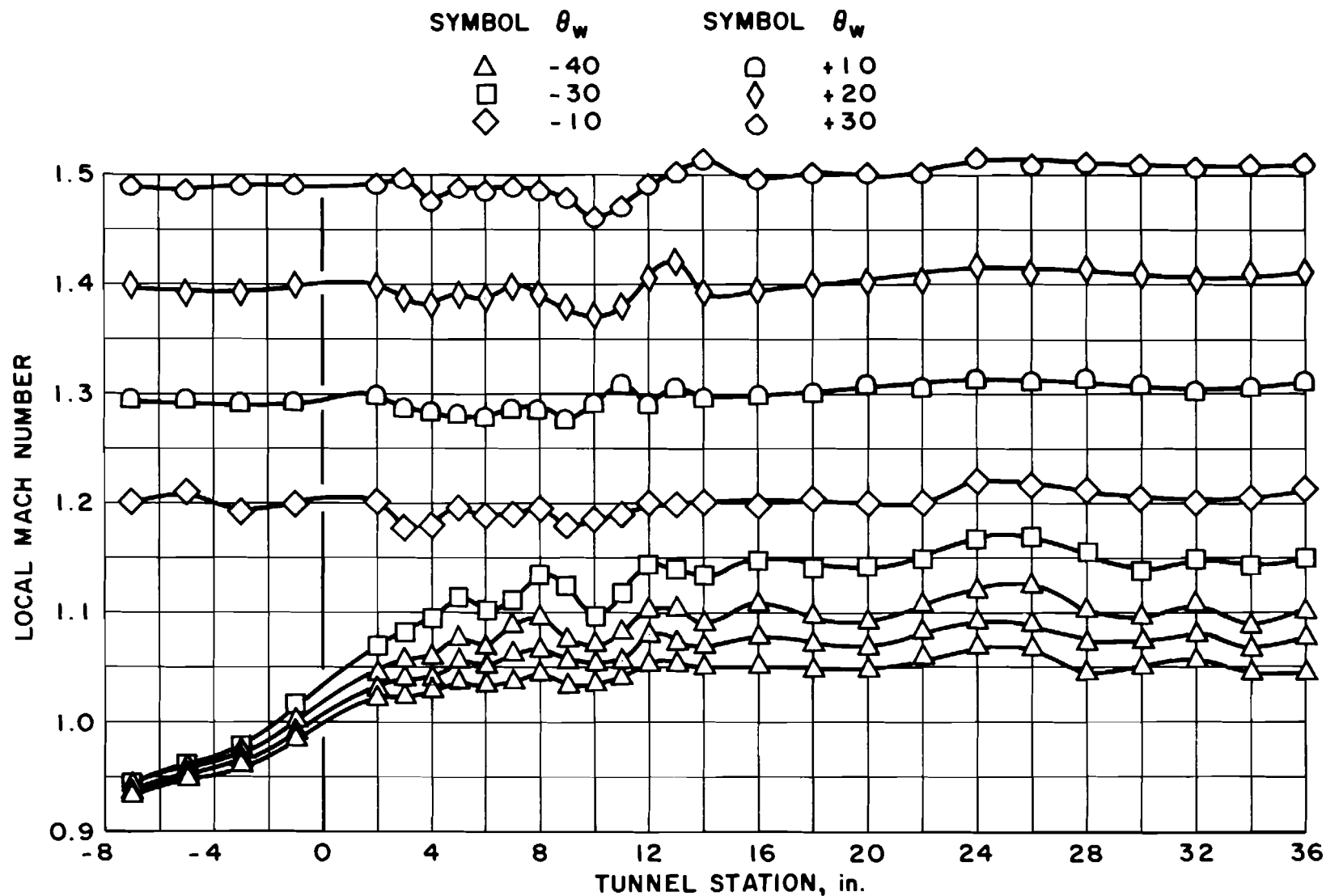
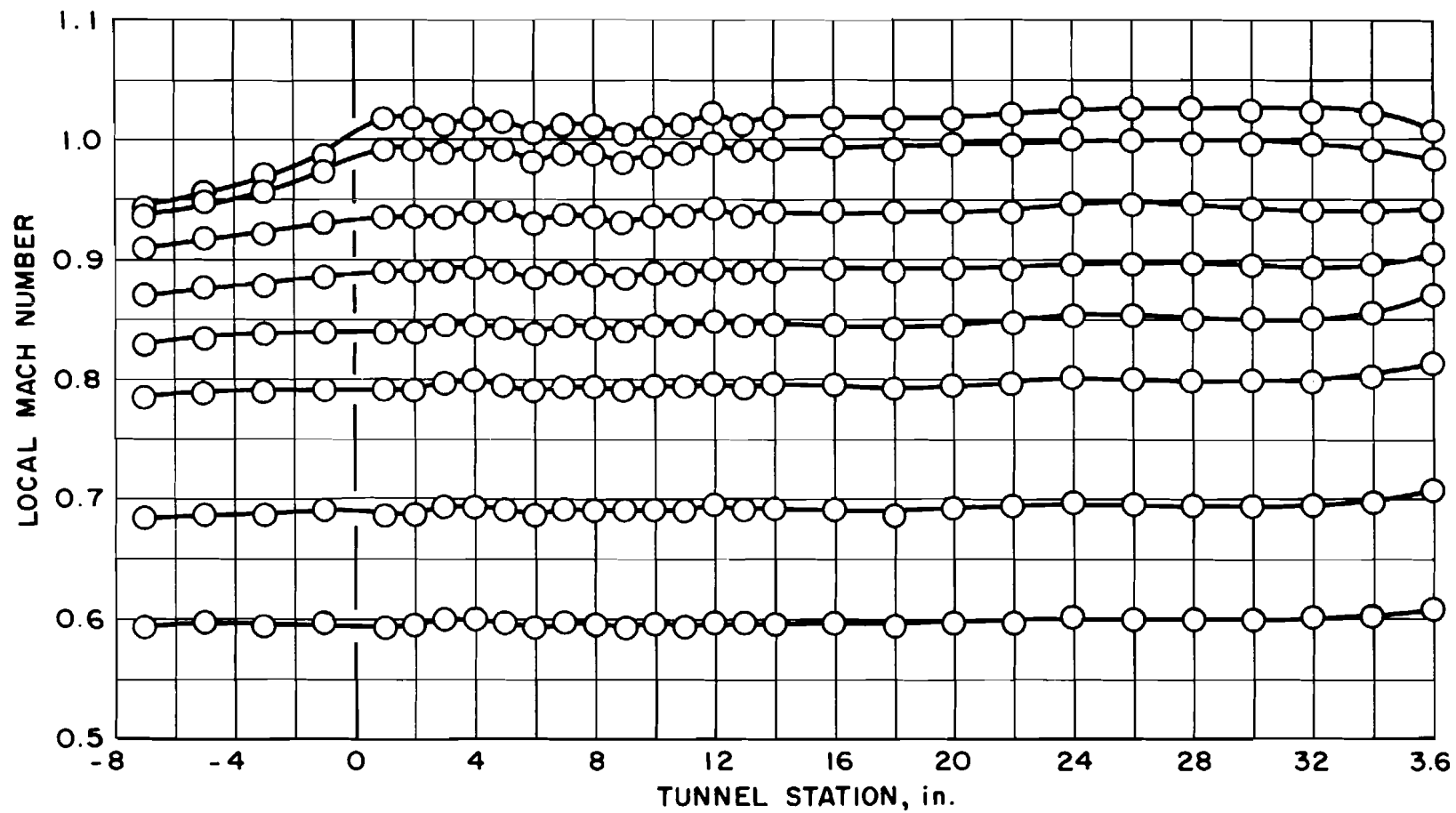


Fig. 9 Top Wall Mach Number Distributions with Four Perforated Test-Section Walls



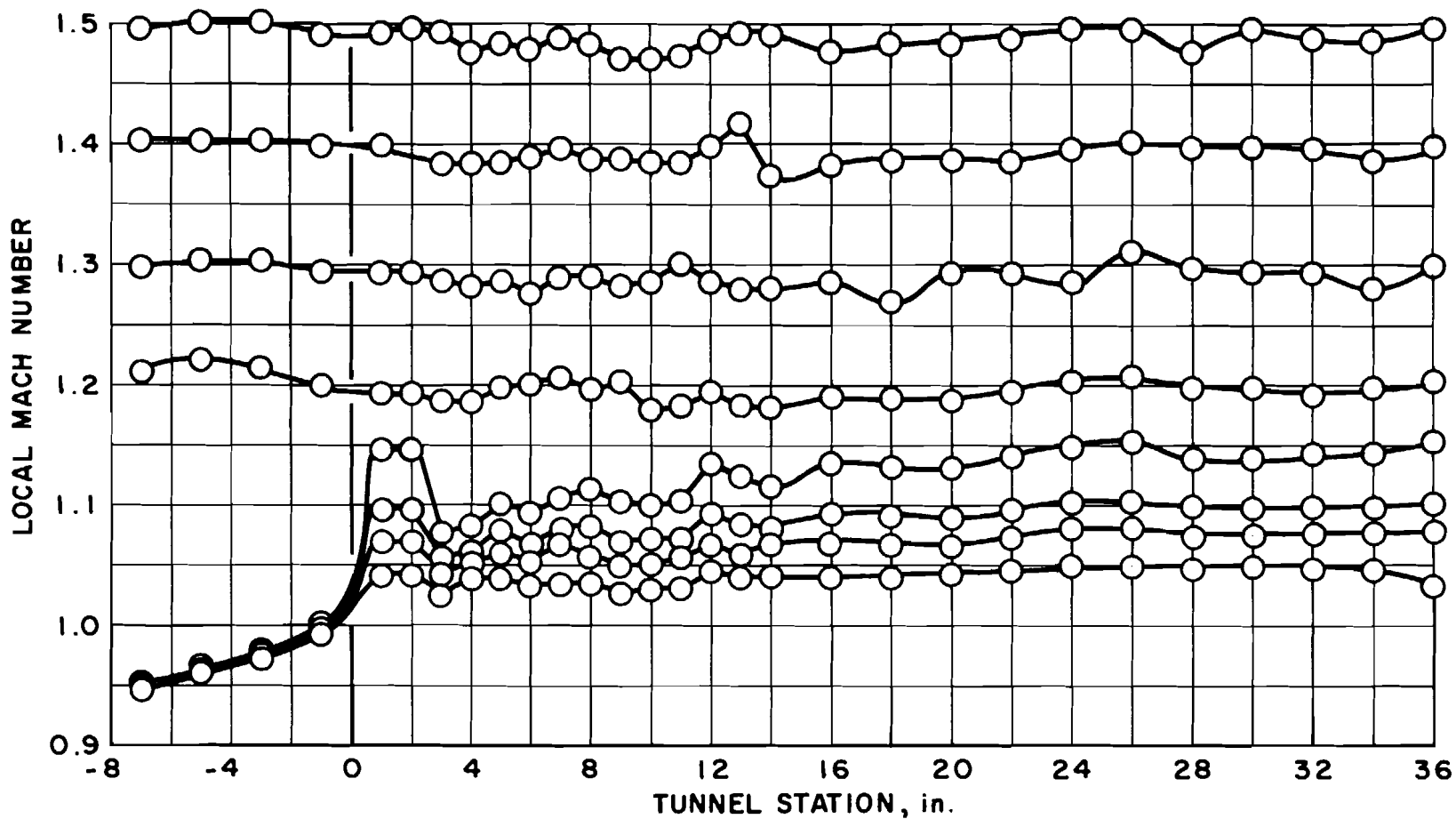
b.  $M = 1.05$  to  $1.50$

Fig. 9 Concluded



$\alpha$ .  $M = 0.60$  to  $1.025$

Fig. 10 Top Wall Mach Number Distributions with Two Perforated Test-Section Walls at  $\theta_w = 0$



b.  $M = 1.05$  to  $1.50$

Fig. 10 Concluded

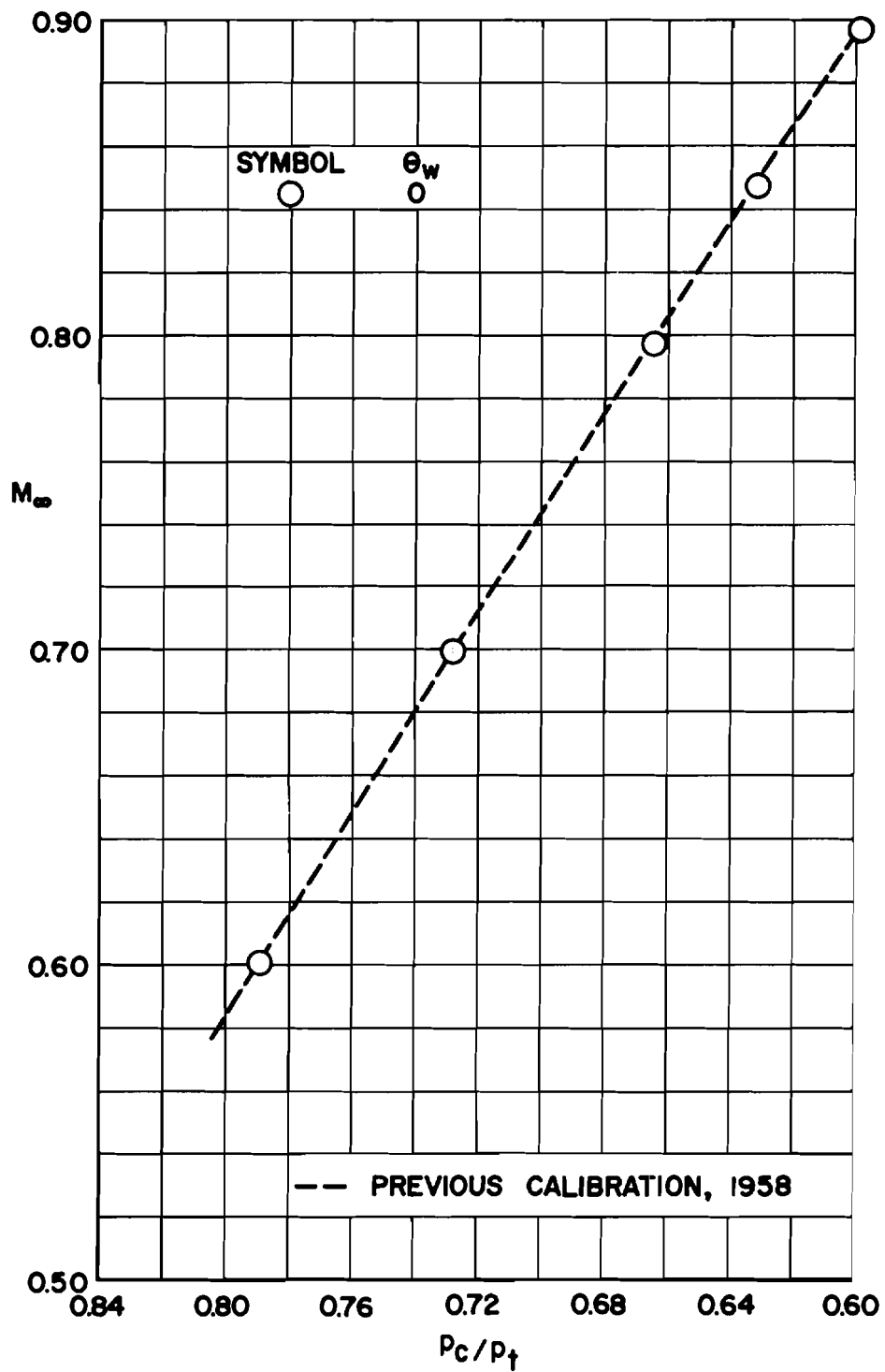


Fig. 11 Comparison of Present and Previous Calibration Results with Four Perforated Test-Section Walls

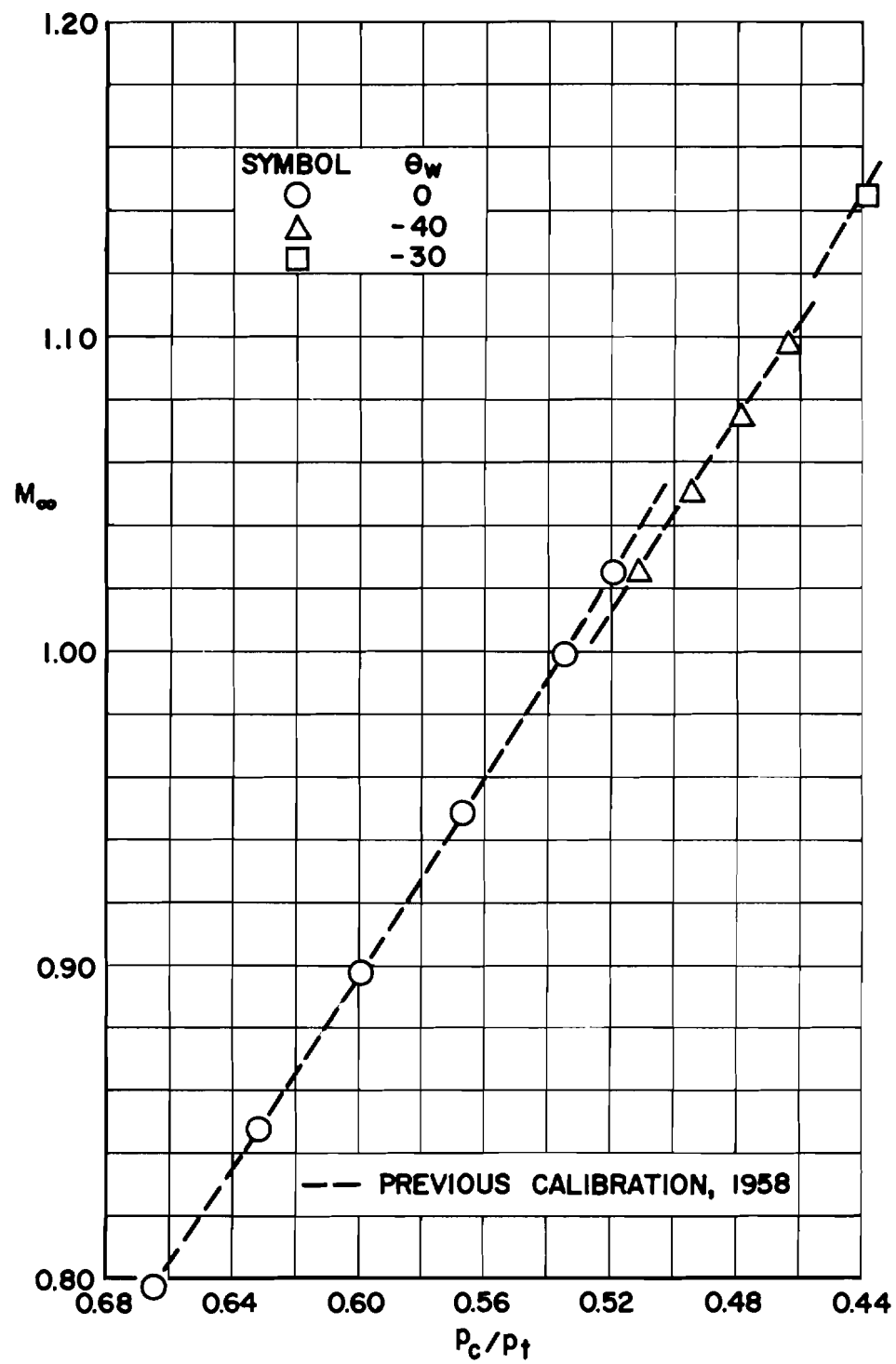


Fig. 11 Continued

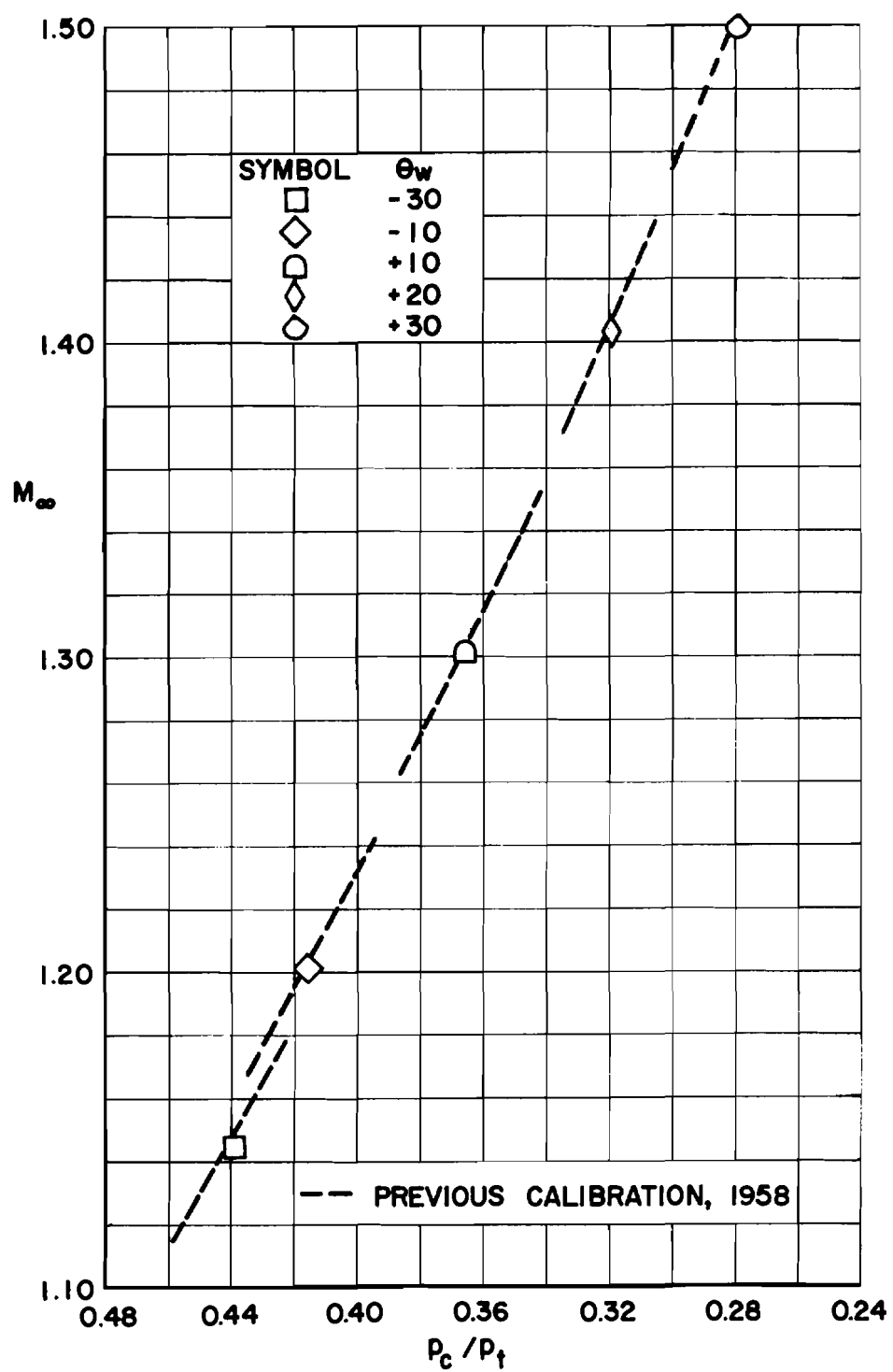


Fig. 11 Concluded



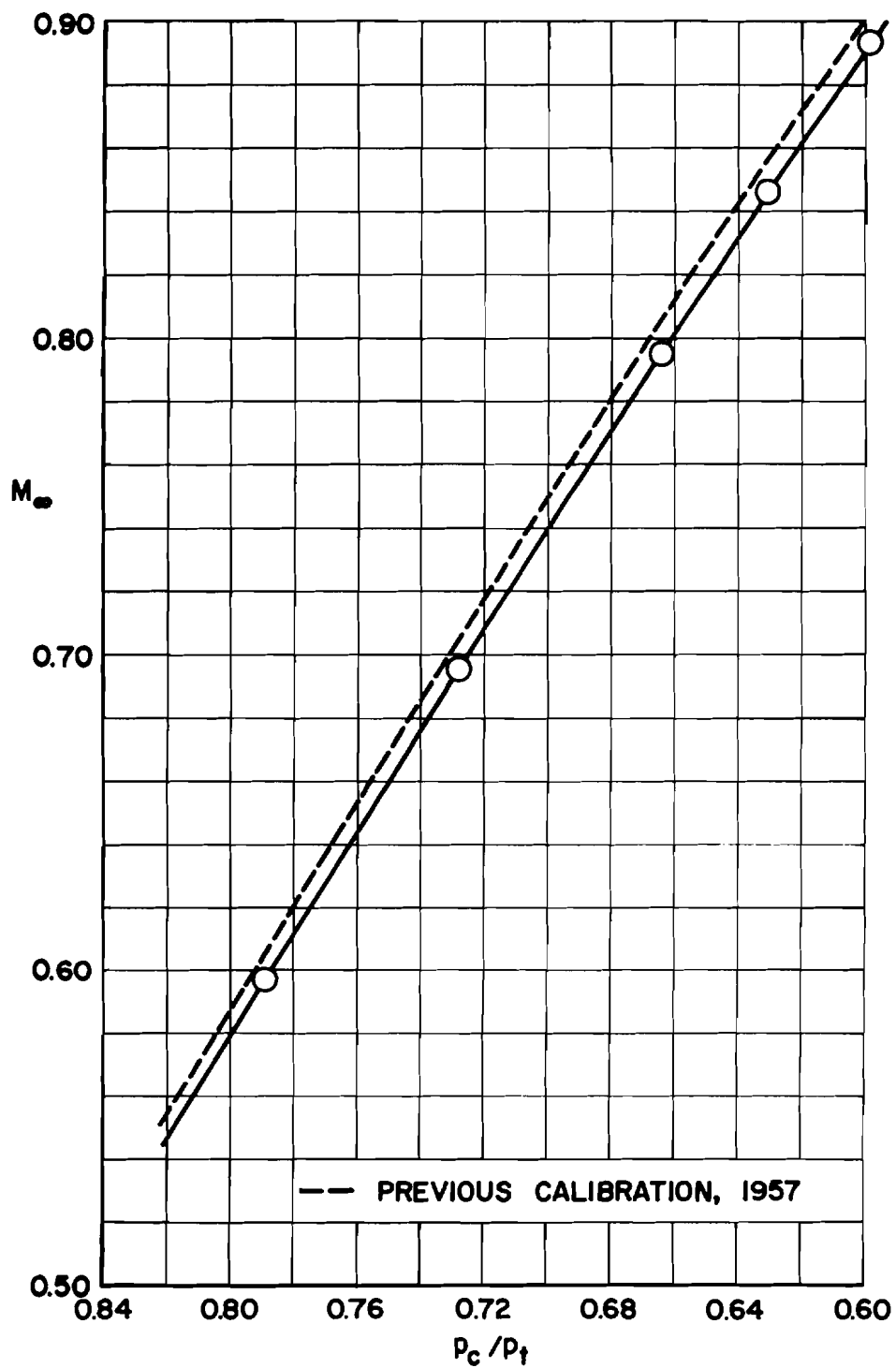


Fig. 12 Comparison of Present and Previous Calibration Results with Two Perforated Test-Section Walls at  $\theta_w = 0$

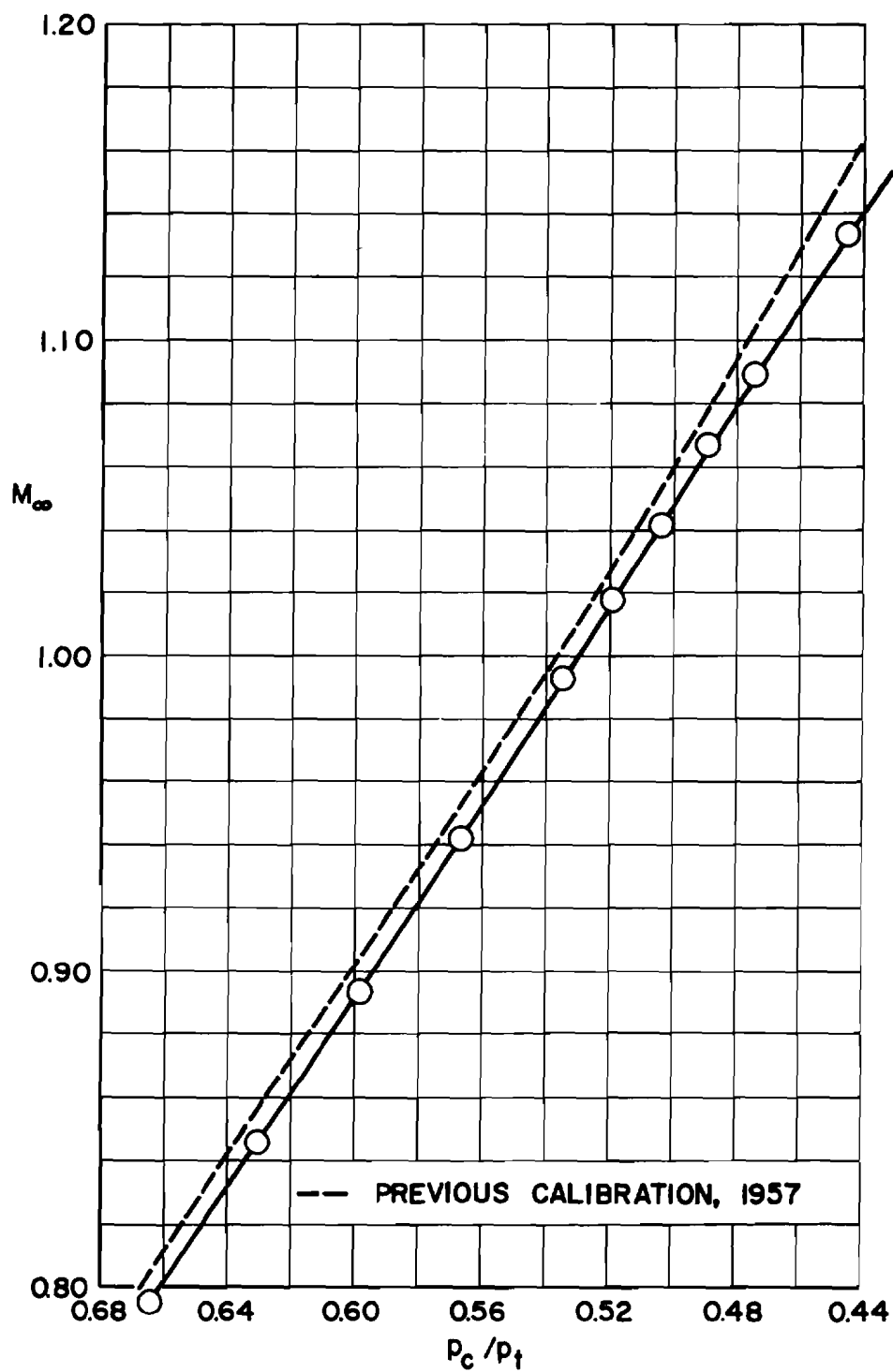


Fig. 12 Continued

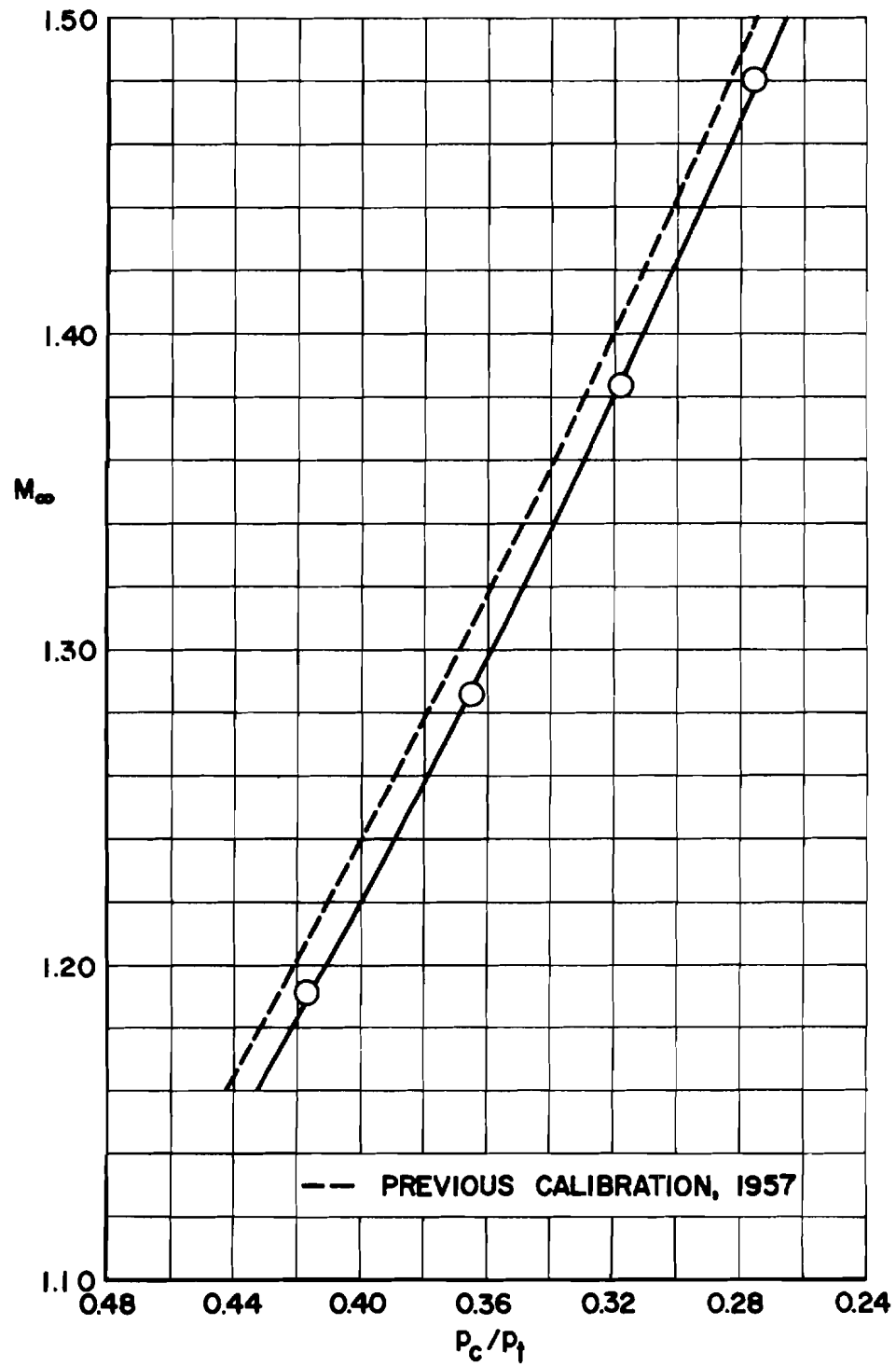


Fig. 12 Concluded

